

Coupling between phonon-phonon and phonon-impurity scattering: A critical revisit of the spectral Matthiessen's rule

Tianli Feng, Bo Qiu, and Xiulin Ruan*

School of Mechanical Engineering and the Birck Nanotechnology Center, Purdue University, West Lafayette, Indiana 47907-2088, USA

(Received 11 November 2014; revised manuscript received 24 November 2015; published 16 December 2015)

The spectral Matthiessen's rule is commonly used to calculate the total phonon scattering rate when multiple scattering mechanisms exist. Here we predict the spectral phonon relaxation time τ of defective bulk silicon using normal mode analysis based on molecular dynamics and show that the spectral Matthiessen's rule is not accurate due to the neglect of the coupling between anharmonic phonon-phonon scattering τ_a^{-1} and phonon-impurity scattering τ_i^{-1} . As a result, the spectral Matthiessen's rule underestimates the total phonon scattering rate and hence overestimates the thermal conductivity κ of mass-doped and Ge-doped silicon by about 20–40%. We have also directly estimated this coupling scattering rate, so-called coupled five-phonon scattering $\tau_{\text{couple}}^{-1}$, and achieved good agreement between $\tau_a^{-1} + \tau_i^{-1} + \tau_{\text{couple}}^{-1}$ and the total scattering rate τ_{tot}^{-1} .

DOI: [10.1103/PhysRevB.92.235206](https://doi.org/10.1103/PhysRevB.92.235206)

PACS number(s): 66.70.Df, 61.72.-y, 63.20.kp, 63.20.kg

The spectral Matthiessen's (M's) rule is a general rule to estimate the total spectral scattering rate when multiple scattering mechanisms exist at the same time [1]. In most solids, phonon transport is governed by phonon-phonon scattering $\tau_{a,\lambda}^{-1}$, phonon-impurity scattering $\tau_{i,\lambda}^{-1}$, phonon-boundary scattering $\tau_{b,\lambda}^{-1}$, etc., where λ specifies a phonon mode $\lambda = (\mathbf{k}, \nu)$ with wave vector \mathbf{k} and dispersion branch ν . By adding all of these factors, the spectral M's rule gives the total scattering rate as $\tau_{\text{tot},\lambda}^{-1} = \tau_{a,\lambda}^{-1} + \tau_{i,\lambda}^{-1} + \tau_{b,\lambda}^{-1} + \dots$. This scattering rate plays a crucial rule in predicting thermal conductivity κ based on the Boltzmann transport equation (BTE) $\kappa_z = \frac{1}{V} \sum_{\lambda} v_{z,\lambda}^2 c_{\lambda} \tau_{\lambda}$, where v_z is the projection of the phonon group velocity along the transport z direction, V is the volume, c_{λ} is phonon specific heat per mode [2], and the summation is done over all the resolvable phonon modes [3]. This approach has been applied to predict the thermal conductivities of isotope-rich semiconductors [4–6], alloys [7–9], nanostructures [10,11], etc. [12]. However, as an empirical rule, the M's rule assumes that the scattering mechanisms are independent, which was usually not verified in those calculations employing them. The spectral M's rule has not been examined yet, although the failures of the conventional gray M's Rules, i.e., $\sum \mu_j^{-1} = \mu_{\text{tot}}^{-1}$ or $\sum \sigma_j^{-1} = \sigma_{\text{tot}}^{-1}$ for electrical transport [1,13] and $\sum \Lambda_j^{-1} = \Lambda_{\text{tot}}^{-1}$ or $\sum \kappa_j^{-1} = \kappa_{\text{tot}}^{-1}$ for phonon transport [14,15] have been studied extensively, where μ , σ , and Λ are the electron mobility, electrical conductivity, and effective phonon mean free path, respectively. Take phonon transport for instance, the correct approach is to first obtain the spectral total relaxation time using the spectral M's rule $\tau_{\text{tot},\lambda}^{-1} = \sum_j \tau_{j,\lambda}^{-1}$ and then derive the thermal conductivity using the Boltzmann transport equation (BTE) $\kappa_{\text{tot}} \sim \int c(\omega) v_g(\omega) / v_p^2(\omega) \omega^2 \tau_{\text{tot},\lambda}(\omega) d\omega$, where c , v_g , and v_p are the phonon specific heat, group velocity, and phase velocity, respectively. It can be conveniently shown that only if all the τ_j 's have the same ω dependence, one can first use BTE to obtain the partial thermal conductivity due to one scattering mechanism $\kappa_j \sim \int c(\omega) v_g(\omega) / v_p^2(\omega) \omega^2 \tau_{j,\lambda}(\omega) d\omega$

and then use the gray M's rule to obtain the same total thermal conductivity $\kappa_{\text{tot}}^{-1} = \sum_j \kappa_j^{-1}$, i.e., the gray M's rule is valid. However, in general the τ_j 's have different ω dependencies. Therefore, the failure of the gray M's rule can be expected, while the spectral M's rule has been assumed to be valid all the time. Thus in this paper, our objectives are to (1) predict the spectral phonon scattering rate $\tau_{\text{tot},\lambda}^{-1}$ and thermal conductivity κ without touching the detailed phonon scattering processes or the spectral M's rule, and (2) examine the accuracy of the spectral M's rule and provide physical interpretation and quantitative correction.

We take defective bulk Si as an example and calculate $\tau_{a,\lambda}^{-1}$, $\tau_{i,\lambda}^{-1}$, and $\tau_{\text{tot},\lambda}^{-1}$ in three independent ways. $\tau_{a,\lambda}^{-1}$ is obtained by performing the phonon normal mode analysis (NMA) [12,16–21] on pristine silicon, in which only phonon-phonon scattering occurs. $\tau_{i,\lambda}^{-1}$ is calculated from the Tamura's formalism, and $\tau_{\text{tot},\lambda}^{-1}$ is calculated by NMA on the defective silicon. The spectral M's rule is examined by comparing $\tau_{a,\lambda}^{-1} + \tau_{i,\lambda}^{-1}$ to $\tau_{\text{tot},\lambda}^{-1}$. To examine the accuracy of these scattering rates, we compare the thermal conductivity κ predicted from $\tau_{a,\lambda}^{-1} + \tau_{i,\lambda}^{-1}$ or $\tau_{\text{tot},\lambda}^{-1}$ with that from the Green-Kubo method based on MD. The scattering rates $\tau_{a,\lambda}^{-1}$ and $\tau_{\text{tot},\lambda}^{-1}$ were obtained by performing the following NMA on pristine silicon and on defective silicon, respectively,

$$q_{\lambda}(t) = \sum_{\alpha} \sum_b^n \sum_l^{N_c} \sqrt{\frac{m_b}{N_c}} u_{\alpha}^{l,b}(t) e_{b,\alpha}^{\lambda*} \exp[i\mathbf{k} \cdot \mathbf{r}_0^l], \quad (1)$$

$$\Phi_{\lambda}(\omega) = |\mathcal{F}[\dot{q}_{\lambda}(t)]|^2 = \frac{C_{\lambda}}{(\omega - \omega_{\lambda}^A)^2 + (\tau_{\lambda}^{-1})^2/4}. \quad (2)$$

Here, $u_{\alpha}^{l,b}(t)$ is the α th component of the time dependent displacement of the b th basis atom in the l th unit cell, e is the phonon eigenvector, \mathbf{r}_0 is the equilibrium position, \mathcal{F} denotes the Fourier transformation, and $\Phi_{\lambda}(\omega)$ is called spectral energy density. C_{λ} is a constant for a given λ . $\Phi_{\lambda}(\omega)$ is a Lorentzian function with peak position ω_{λ}^A and full width τ_{λ}^{-1} at half maximum. By MD simulation the time dependent atomic velocity \dot{u} is obtained and substituted into Eqs. (1) and (2) to obtain the spectral phonon scattering rate τ_{λ}^{-1} . With

*ruan@purdue.edu

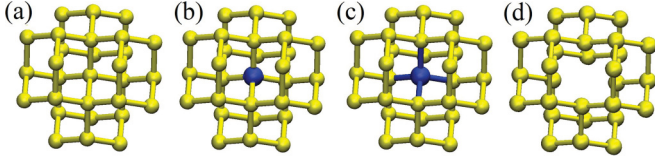


FIG. 1. (Color online) Sketches of the lattice structures of (a) the pristine *c*-Si, (b) the mass-doped *c*-Si (m_i Si-Si), (c) the ^{73}Ge -doped *c*-Si (^{73}Ge -Si), and (d) the vacancy-doped *c*-Si (V-Si).

this method, we can obtain $\tau_{a,\lambda}^{-1}$ of pristine silicon and $\tau_{\text{tot},\lambda}^{-1}$ of impurity-doped silicon independently. In the evaluation of $\tau_{\text{tot},\lambda}^{-1}$, the intrinsic lattice anharmonicity and the extrinsic impurity are treated as a combined perturbation to the phonon normal modes. This method does not touch the details of the scattering processes or the spectral M's rule.

From the second-order perturbation theory [1,22], Tamura gave the isotope scattering rate by Fermi's golden rule (FGR) [23],

$$\tau_{i,\lambda}^{-1} = \frac{\pi}{2N_c} \omega_\lambda^2 \sum_b \sum_{\lambda' \neq \lambda} g_b |\mathbf{e}_b^\lambda \cdot \mathbf{e}_b^{\lambda'*}|^2 \delta(\omega_\lambda - \omega_{\lambda'}), \quad (3)$$

where $g_b = \sum_\beta f_{\beta b} (1 - m_{\beta b}/\bar{m}_b)^2$ characterizes the magnitude of mass disorder, with β , $f_{\beta b}$, and \bar{m}_b indicating the isotope types, the fraction of isotope in the b th basis atom, and the average atom mass at the b th basis. Equation (3) is equivalent to $\pi g \omega_\lambda^2 D(\omega_\lambda)/2$ for cubic lattice structures, where $D(\omega)$ is the normalized density of states. The Tamura's formalism was first derived for the calculation of isotope scattering rate but recently has been applied to many other impurities with bonding change [7–9,24,25]. In the last part of the paper we study the contribution of the impurity bonding strength to the total scattering rate. In the long wavelength approximation (LWA) [22,23,26], Eq. (3) is reduced to the $\sim \omega^4$ relation, $\tau_i^{-1} = \frac{V_c n_c (\Delta m)^2}{4\pi v_g v_p^2 m_c^2} \omega^4$, where V_c is the volume of a unit cell, n_c is the concentration of the impurities, and v_g and v_p are the group and phase velocities of the phonon, respectively.

We investigate the pristine *c*-Si, the mass-doped *c*-Si (m_i Si-Si), the ^{73}Ge -doped *c*-Si (^{73}Ge -Si), and the vacancy-doped *c*-Si (V-Si) bulks [27,28] at classical 300 K with the sketches of the lattice structures shown in Fig. 1. Here the m_i Si-Si is to substitute some of the original Si atoms with mass m_i while keeping the bonds unchanged. The NMA and the Tamura's formalism rely on MD simulations and lattice dynamics (LD) calculations, which are conducted in LAMMPS [29] and GULP [30], respectively. All the scattering rates are calculated based on the Tersoff interatomic potential [31]. The domain size and total simulation time are set as $8 \times 8 \times 8$ conventional cubic cells and 10 ns to eliminate the size and time effects [19]. Each time step is set as $\Delta t = 0.5$ fs to resolve all the phonon modes. From the simulation results, it is found that one impurity affects at most the motions of its nearest (2.3 Å) and second nearest (3.8 Å) neighbors because of the approximate tight binding force in silicon. In our simulation, the impurities were randomly distributed with the distance between each of the two defects being larger than 11 Å to ensure the defects do not influence each other.

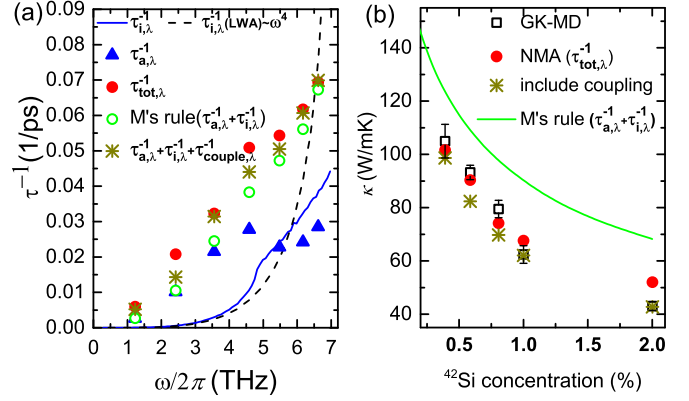


FIG. 2. (Color online) (a) The phonon scattering rates of the TA mode in the [100] direction in pristine *c*-Si and 0.4% ^{42}Si doped silicon. (b) The thermal conductivity of ^{42}Si -Si calculated from four different methods as a function of the ^{42}Si concentration.

Three or more independent simulations are conducted for each case to minimize the statistical error. In the lattice dynamics calculation we employed a \mathbf{k} grid of $96 \times 96 \times 96$ to obtain results as accurately as possible, since Eq. (1) requires the evaluation of delta functions.

Figure 2 (a) gives the phonon scattering rates of the TA mode in the [100] direction for 0.4% ^{42}Si -Si at classical 300 K. The phonon-phonon scattering rate $\tau_{a,\lambda}^{-1}$ scales as $\sim \omega^2$ at low frequencies but deviates at higher frequencies. Such a trend was also seen in previous studies [20,32]. The $\tau_{i,\lambda}^{-1}$ calculated from Eq. (3) is found to be exactly the same with $\pi g \omega_\lambda^2 D(\omega_\lambda)/2$ as mentioned above. At low frequency, τ_i^{-1} is about one order of magnitude lower than τ_a^{-1} . As the frequency increases, τ_i^{-1} becomes even higher than τ_a^{-1} due to the increase of the density of states. We also note that the impurity scattering rate obeys the $\sim \omega^4$ relation given by the LWA (dashed black line) for the phonon frequency below 1.5 THz. For higher frequency where phonon wavelength is short and comparable with the defect size, the Rayleigh scattering model breaks down giving way to the Mie scattering model, and thus the $\sim \omega^4$ frequency dependence gradually fades with increasing frequency [33]. Interestingly, we find that the spectral M's rule, $\tau_a^{-1} + \tau_i^{-1}$ (open green circle), underestimates the phonon total scattering rates (solid red circle) by 10–50% for different frequencies. To ensure this discrepancy is not due to the different domain sizes used in the NMA and Tamura's formula, we have performed both the MD simulations and FGR calculations in the domain of $16 \times 16 \times 16$ unit cells and the same-size \mathbf{k} mesh, respectively. We have found that such discrepancy indeed exists, especially in the mid-frequency range. Actually the impurity scattering rates do not vary much when the \mathbf{k} -mesh size changes from $96 \times 96 \times 96$ to $16 \times 16 \times 16$ since the latter is already dense enough to obtain a good phonon density of states. In our work, all the calculations are done based on the same Tersoff potential, and the comparison between the results of different methods is self-consistent. Thus, the conclusions still hold although the dispersion has discrepancy with experiments.

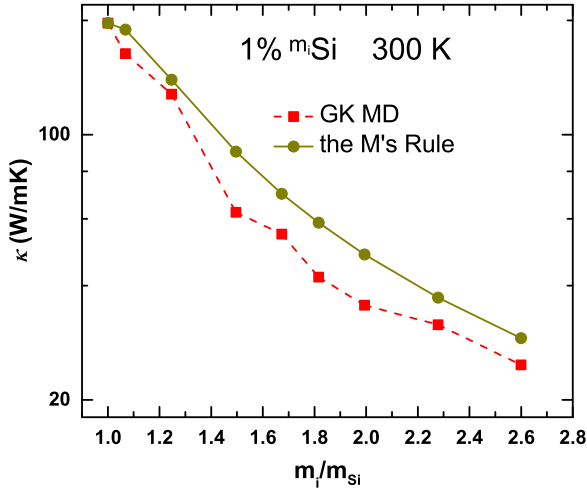


FIG. 3. (Color online) The comparison of the thermal conductivity calculated from GK-MD and the M's rule for 1% m_i Si-Si at classical 300 K.

The thermal conductivity κ as a function of the ^{42}Si concentration at classical 300 K is shown in Fig. 2(b). The NMA and GK are both based on classical equilibrium molecular dynamics and the same interatomic potential. In our calculation results, their agreement is good (within 5%). As seen in Fig. 2(b) for the mass doped bulk silicon, the NMA thermal conductivity values (red circles) match excellently with GK values (black squares). For pristine c -Si, our Green-Kubo and NMA methods give consistent thermal conductivity values. In contrast, the κ calculated from the spectral M's rule [green line] has about 20–40% overestimation. This overestimation has also been observed in the doped silicon with a broad range of mass (28–73) at a concentration of 1%, as seen in Fig. 3.

The physical mechanism for the inaccuracy of the spectral M's rule is explored from the second-order perturbation theory [34]. The phonon scattering operator and rate for a defective material are described as

$$H_{\text{scatt}} = H_a + H_i + (H_a + H_i)(E + H_0 + i\varepsilon)^{-1}(H_a + H_i), \quad (4)$$

$$\tau_{\text{tot},\lambda}^{-1} = \tau_{a,\lambda}^{-1} + \tau_{i,\lambda}^{-1} + \tau_{\text{couple},\lambda}^{-1}, \quad (5)$$

where H_0 is the harmonic lattice Hamiltonian, and ε is a positive infinitesimal [34]. The first two terms H_a and H_i are the perturbation Hamiltonians from intrinsic anharmonicity and extrinsic impurity, leading to intrinsic anharmonic phonon-phonon scattering $\tau_{a,\lambda}^{-1}$ and extrinsic phonon-impurity scattering $\tau_{i,\lambda}^{-1}$, respectively. The former includes the intrinsic three-phonon, four-phonon, five-phonon processes, etc., and the latter involves two phonons. The third operator in Eq. (4), which was usually ignored by researchers, represents the coupling between H_a and H_i and may involve five or more phonons. To the lowest order of the coupling, the coupled five-phonon scattering (three phonons in three-phonon scattering and the two phonons in the impurity scattering) provides additional channels for one mode to scatter to the other mode and thus increases the scattering rate, as shown in

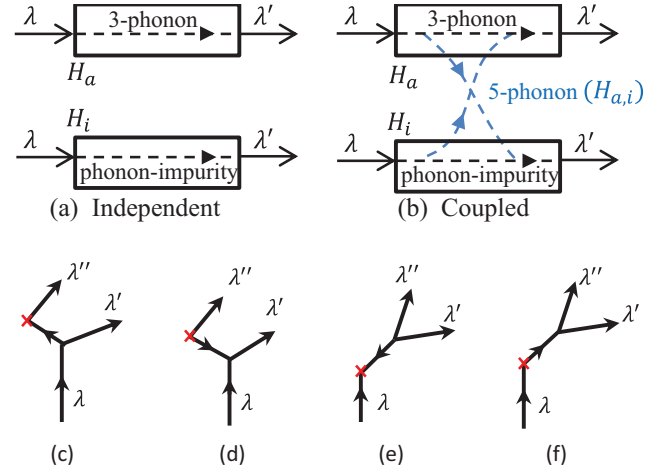


FIG. 4. (Color online) Brief sketches for illustrating (a) the independent scattering mechanisms and (b) the coupled scattering mechanisms. The sketches of coupling scattering are (c), (d), (e), and (f) with detailed descriptions found in Refs. [34,35]. The \times represents the scattering by impurity.

Figs. 4(a) and 4(b). The detailed sketches for the coupled five-phonon process are shown in Figs. 4(c)–4(f). Note that this coupled five-phonon process is different from the intrinsic five-phonon process which has already been included in the term $\tau_{a,\lambda}^{-1}$. The term “coupling” is used because the transitions occur between the intermediate quantum states of the three-phonon process and impurity-phonon process with detailed sketches shown in Refs. [34,35]. This coupling is calculated by the second-order perturbation theory and is different from the meaning of “interplay” discussed in Refs. [36,37] where the spectral M's rule was still used [38].

To roughly estimate the contribution of the coupled five-phonon scattering, we applied the approximate expression derived by Carruthers from Fermi's golden rule [34],

$$\tau_{\text{couple},\lambda}^{-1} = \frac{3g}{4} \left(3 \left(\frac{\omega}{\Delta\omega} \right)^2 + \frac{3}{4} + \frac{6\pi\bar{\omega}^4}{\tau_{\text{tot},\lambda}^{-1}\omega_0^3} \right) \tau_{a,\lambda}^{-1}, \quad (6)$$

where $\Delta\omega$ measures “the ‘lack’ of energy conservation by the intermediate phonons” [34] in the five-phonon process, and ω_0 is Debye frequency [39]. This coupled five-phonon scattering rate, however, has, to our knowledge, never been evaluated. We substitute the τ_{tot}^{-1} obtained from NMA into Eq. (6) to estimate the coupling scattering $\tau_{\text{couple},\lambda}^{-1}$ and check the agreement between $\tau_{\text{tot},\lambda}^{-1}$ and $\tau_{a,\lambda}^{-1} + \tau_{i,\lambda}^{-1} + \tau_{\text{couple},\lambda}^{-1}$. By including the estimated coupling scattering rate $\tau_{\text{couple},\lambda}^{-1}$, a good agreement is achieved for both τ and κ as seen in Fig. 2. The frequency dependence of $\tau_{\text{couple},\lambda}^{-1}$ in Fig. 2(a) is explained by Eq. (6) as follows. At low frequencies (1–5 THz), $\tau_{\text{couple},\lambda}^{-1}$ increases with frequency due to the increasing $\tau_{a,\lambda}^{-1}$, while at higher frequencies (6–7 THz), it decreases with frequency since the increasing $\tau_{\text{tot},\lambda}^{-1}$ brings down the third term in the bracket. Physically, at higher frequencies the large density of states allows phonon states to transit into other states quickly by impurity scattering, and thus the intermediate states required in the coupling scattering are probably difficult to produce. Generally, the maximum $\tau_{a,\lambda}^{-1}$ occurs at the mid-frequencies

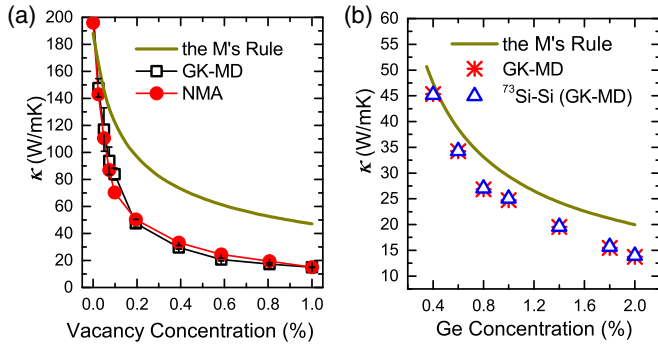


FIG. 5. (Color online) Thermal conductivity of (a) V-Si and (b) ^{73}Ge -Si calculated from GK-MD, NMA, and the spectral M's rule as a function of vacancy or Ge concentration at classical 300 K. The blue triangles label κ 's of ^{73}Si -Si as references.

where the phonons have relatively high $\tau_{a,\lambda}^{-1}$ as well as low density of states.

Figure 5(a) shows κ of V-Si as a function of vacancy concentration calculated from different methods. We find that even for bond-missing defects our NMA (red circle) presents excellent agreement with GK-MD (black square), indicating that treating the impurities and anharmonicity as one combined perturbation to calculate total scattering rates is reasonable. The spectral M's rule (yellow line) overpredicts κ of V-Si by about 100–150% at a vacancy concentration of 0.2–1%. The discrepancy comes from two aspects: (1) the spectral M's rule neglects the coupling between phonon-phonon and phonon-defect scattering rates as elaborated earlier, and (2) the Tamura's formalism only captures the scattering by mass disorder while ignoring the bond changes. As for ^{73}Ge -Si shown in Fig. 5(b), the spectral M's rule overpredicts about 20–40% of κ . Most of this discrepancy comes from the coupling, since we find that ^{73}Ge -Si and ^{73}Si -Si have almost the same thermal conductivity, indicating that the Ge-Si bond provides negligible scattering compared to the mass disorder introduced by Ge atoms. In addition, the overprediction of κ by the spectral M's rule is also seen in the high Ge concentration range [34,40].

For two materials having the same light-doping level ($\tau_{i,\lambda}^{-1} \ll \tau_{a,\lambda}^{-1}$), the coupling strength, defined by $\tau_{\text{couple},\lambda}^{-1}/\tau_{\text{tot},\lambda}^{-1}$, is approximately $1/\tau_{a,\lambda}^{-1}$ and is higher for the higher- κ material which has a lower $\tau_{a,\lambda}^{-1}$. On the other hand, if the doping level is high ($\tau_{i,\lambda}^{-1} \gg \tau_{a,\lambda}^{-1}$), the coupling strength $\sim \tau_{a,\lambda}^{-1}/\tau_{i,\lambda}^{-1}$ is higher for the lower- κ material which has a higher $\tau_{a,\lambda}^{-1}$.

For general materials, the phonon scattering rates as a function of doping concentration are shown in Fig. 6. The coupling scattering rate initially increases rapidly with doping in the light doping regime and then increases linearly and more slowly in the heavy doping regime. As a result, a maximum of the coupling strength occurs when the system transits from the light to heavy doping. For example, for silicon doped with Ge in our work as shown in Fig. 5(b), the coupling strength increases to 0.4 as the doping level increases to 2%. On the other hand, at the concentration of 50% which is in the alloy limit, the coupling strength is

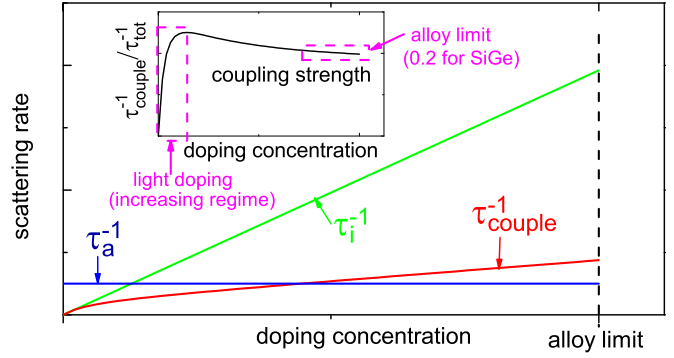


FIG. 6. (Color online) A sketch to show the scattering rates and the coupling effect (inset) as a function of doping level.

about $\tau_{\text{couple}}^{-1}/\tau_{\text{tot}}^{-1} \approx 4\tau_a^{-1}/\tau_{\text{tot}}^{-1} \approx 4(1/156)/(1/7) \approx 0.2$. Here we used the approximation of $\tau_{\text{couple}}^{-1} \approx 10g\tau_a^{-1}$ [34] with $g \approx 0.4$ in SiGe alloy and the fact that pristine silicon and SiGe alloy have the thermal conductivities of 156 W/mK and 7 W/mK, respectively. Carruthers *et al.* hypothesized that this coupled-five-phonon scattering caused the overestimation of the thermal conductivity of SiGe alloy in early years [34,40], though a quantitative evaluation was not done in their work. The concept of the coupling effect can be extended to all doped material systems, and the general trends should be similar to Fig. 6. For example, the coupling strength in PbTe/Se alloy is estimated to be about 9%, which may account for the overestimation in Ref. [9]. In Ref. [7], Garg *et al.* included the coupling implicitly by calculating the three-phonon scattering rates in a large SiGe alloy supercell using fully-quantum density functional perturbation theory. Although the five-phonon processes were implicitly included in prior calculations of the total phonon scattering rates, we have isolated the scattering rate due to five-phonon processes only.

To conclude, without touching the details of the phonon scattering processes, we have used the NMA approach to predict the thermal properties of defective materials more accurately than the spectral M's rule. The spectral M's rule is found to overpredict the phonon relaxation time and thermal conductivity because the spectral M's rule does not take into account the coupling between anharmonic phonon-phonon scattering and impurity scattering. Our results demonstrate one system which has strong coupling between different scattering mechanisms and estimate the coupling scattering rates with good quantitative accuracy. Such coupling exists in many different systems of solids and can be explored for lower κ as well as higher ZT for thermoelectrics.

We would like to thank Ajit Vallabhaneni and Frank Brown for proofreading the manuscript, and Yan Wang for helpful discussions. Simulations were performed at the Purdue Network for Computational Nanotechnology (NCN). The work was supported by the National Science Foundation (Award No. 1150948).

- [1] J. M. Ziman, *Electrons and Phonons* (Oxford University Press, London, 1960).
- [2] To be consistent with the GK method based classical MD simulations, in this paper the value of c_λ is taken as k_B under the classical Boltzmann distribution.
- [3] J. E. Turney, E. S. Landry, A. J. H. McGaughey, and C. H. Amon, *Phys. Rev. B* **79**, 064301 (2009).
- [4] L. Lindsay, D. A. Broido, and T. L. Reinecke, *Phys. Rev. B* **87**, 165201 (2013).
- [5] L. Lindsay and D. A. Broido, *J. Phys.: Condens. Matter* **20**, 165209 (2008).
- [6] L. Lindsay, D. A. Broido, and T. L. Reinecke, *Phys. Rev. Lett.* **109**, 095901 (2012).
- [7] J. Garg, N. Bonini, B. Kozinsky, and N. Marzari, *Phys. Rev. Lett.* **106**, 045901 (2011).
- [8] Y. He, I. Savić, D. Donadio, and G. Galli, *Phys. Chem. Chem. Phys.* **14**, 16209 (2012).
- [9] Z. Tian, J. Garg, K. Esfarjani, T. Shiga, J. Shiomi, and G. Chen, *Phys. Rev. B* **85**, 184303 (2012).
- [10] N. Mingo and L. Yang, *Phys. Rev. B* **68**, 245406 (2003).
- [11] P. Martin, Z. Aksamija, E. Pop, and U. Ravaioli, *Phys. Rev. Lett.* **102**, 125503 (2009).
- [12] T. Feng and X. Ruan, *J. Nanomaterials* **2014**, 206370 (2014).
- [13] Y. Takeda and T. P. Pearsall, *Electron. Lett.* **17**, 573 (1981).
- [14] J. E. Turney, A. J. H. McGaughey, and C. H. Amon, *J. Appl. Phys.* **107**, 024317 (2010).
- [15] M. Luisier, *Appl. Phys. Lett.* **103**, 113103 (2013).
- [16] J. A. Thomas, J. E. Turney, R. M. Iutzi, C. H. Amon, and A. J. H. McGaughey, *Phys. Rev. B* **81**, 081411 (2010).
- [17] A. J. C. Ladd, B. Moran, and W. G. Hoover, *Phys. Rev. B* **34**, 5058 (1986).
- [18] N. de Koker, *Phys. Rev. Lett.* **103**, 125902 (2009).
- [19] A. J. H. McGaughey and M. Kaviani, *Phys. Rev. B* **69**, 094303 (2004).
- [20] A. S. Henry and G. Chen, *J. Comput. Theor. Nanosci.* **5**, 141 (2008).
- [21] T. Feng, B. Qiu, and X. Ruan, *J. Appl. Phys.* **117**, 195102 (2015).
- [22] P. Klemens, *Solid State Physics*, Vol. 7 (Academic Press Inc., New York, USA, 1958).
- [23] S.-i. Tamura, *Phys. Rev. B* **27**, 858 (1983).
- [24] A. Kundu, N. Mingo, D. A. Broido, and D. A. Stewart, *Phys. Rev. B* **84**, 125426 (2011).
- [25] W. Li, L. Lindsay, D. A. Broido, D. A. Stewart, and N. Mingo, *Phys. Rev. B* **86**, 174307 (2012).
- [26] M. Kaviani, *Heat Transfer Physics* (Cambridge University Press, New York, 2008).
- [27] T. Shiga, T. Hori, and J. Shiomi, *Jpn. J. Appl. Phys.* **53**, 021802 (2014).
- [28] T. Wang, G. K. H. Madsen, and A. Hartmaier, *Modell. Simul. Mater. Sci. Eng.* **22**, 035011 (2014).
- [29] S. Plimpton, *J. Comput. Phys.* **117**, 1 (1995).
- [30] J. D. Gale, *J. Chem. Soc., Faraday Trans.* **93**, 629 (1997).
- [31] J. Tersoff, *Phys. Rev. B* **39**, 5566 (1989).
- [32] K. Esfarjani, G. Chen, and H. T. Stokes, *Phys. Rev. B* **84**, 085204 (2011).
- [33] P. G. Klemens, *Proc. Phys. Soc., London, Sect. A* **68**, 1113 (1955).
- [34] P. Carruthers, *Phys. Rev.* **125**, 123 (1962).
- [35] P. Carruthers, *Rev. Mod. Phys.* **33**, 92 (1961).
- [36] L. Lindsay, D. A. Broido, and T. L. Reinecke, *Phys. Rev. B* **88**, 144306 (2013).
- [37] L. Lindsay and D. A. Broido, *Phys. Rev. B* **85**, 035436 (2012).
- [38] The interplay between isotope scattering and 3-phonon scattering was studied for heavily doped beryllium-VI compounds [36] and boron nitride [37]. There it was illustrated that the highly doped isotopes changed the phonon dispersion relation and further influenced the 3-phonon scattering rate. In their approach, although H_a is modified due to the doping of isotopes, H_a and H_i were evaluated separately, and no coupling between them was included. Thus, the spectral M's rule was still used.
- [39] A detailed explanation of these parameters is found in Ref. [34] online, according to which $\omega/\Delta\omega$, ω_0 , and $\bar{\omega}$ are roughly taken as 2, $2\pi \times 13$ rad/ps, and $\omega_0/2$, respectively. To roughly estimate the contribution of 5-phonon scattering, the choices of these parameters allow slight changes which will not influence the magnitudes or properties of the final results.
- [40] B. Abeles, D. Beers, G. Cody, and J. Dismukes, *Phys. Rev.* **125**, 44 (1962).